



OPEN

## Design and implementation of an illumination system to mimic skyglow at ecosystem level in a large-scale lake enclosure facility

Andreas Jechow<sup>1,2,3</sup>✉, Günther Schreck<sup>1,2</sup>, Christopher C. M. Kyba<sup>1,3</sup>, Stella A. Berger<sup>1,2,4</sup>, Lukas Thuile Bistarelli<sup>1</sup>, Matthias Bodenlos<sup>2</sup>, Mark O. Gessner<sup>1,2,4,5</sup>, Hans-Peter Grossart<sup>1,2,4,6</sup>, Franziska Kupprat<sup>1</sup>, Jens C. Nejtgaard<sup>1,2,4</sup>, Andreas Pansch<sup>2</sup>, Armin Penske<sup>2</sup>, Michael Sachtleben<sup>2</sup>, Tom Shatwell<sup>1,7</sup>, Gabriel A. Singer<sup>1,8</sup>, Susanne Stephan<sup>2,5</sup>, Tim J. W. Walles<sup>2,4,5</sup>, Sabine Wollrab<sup>1,2,4</sup>, Karolina M. Zielinska-Dabkowska<sup>1,9</sup> & Franz Hölker<sup>1,10</sup>

Light pollution is an environmental stressor of global extent that is growing exponentially in area and intensity. Artificial skyglow, a form of light pollution with large range, is hypothesized to have environmental impact at ecosystem level. However, testing the impact of skyglow at large scales and in a controlled fashion under in situ conditions has remained elusive so far. Here we present the first experimental setup to mimic skyglow at ecosystem level outdoors in an aquatic environment. Spatially diffuse and homogeneous surface illumination that is adjustable between 0.01 and 10 lx, resembling rural to urban skyglow levels, was achieved with white light-emitting diodes at a large-scale lake enclosure facility. The illumination system was enabled by optical modeling with Monte-Carlo raytracing and validated by measurements. Our method can be adapted to other outdoor and indoor skyglow experiments, urgently needed to understand the impact of skyglow on ecosystems.

Emissions of artificial light at night (ALAN) have dramatically increased since the early twentieth century, and current growth rates of lit area and light intensities on Earth exceed 2% per year at the global scale<sup>1</sup>. ALAN makes it possible to extend human activities (both indoor and outdoor) into the night, and is associated with wealth and safety, rendering public perception of ALAN overwhelmingly positive<sup>2</sup>. However, long aware of the artificially increasing brightness of night skies, astronomers have recognized negative aspects of ALAN, pointing to the ‘dark side’ of light emissions by coining the term light pollution<sup>3</sup>. Impacts of ALAN on life were also recognized early on<sup>4</sup>, but detailed investigation of the impact of ALAN on life only began during the last two decades<sup>5–8</sup> showing effects on species level ranging from microorganisms<sup>9</sup> to mammals<sup>10</sup> as well as on important ecosystem services such as pollination<sup>11</sup>. Because humans tend to settle near water bodies<sup>12</sup>, aquatic environments are particularly affected by ALAN, but are currently understudied compared to terrestrial ones<sup>9,13–15</sup>.

<sup>1</sup>Department of Ecohydrology, Leibniz Institute of Freshwater Ecology and Inland Fisheries (IGB), Müggelseedamm 310, 12587 Berlin, Germany. <sup>2</sup>Department of Experimental Limnology, Leibniz Institute of Freshwater Ecology and Inland Fisheries (IGB), Alte Fischerhütte 2, 16775 Stechlin, Germany. <sup>3</sup>Remote Sensing and Geoinformatics Section, Helmholtz Center Potsdam, German Center for Geosciences (GFZ), Telegraphenberg, 14473 Potsdam, Germany. <sup>4</sup>Berlin-Brandenburg Institute of Advanced Biodiversity Research (BBIB), Königin-Luise-Str. 2-4, 14195 Berlin, Germany. <sup>5</sup>Department of Ecology, Berlin Institute of Technology (TU Berlin), Ernst-Reuter-Platz 1, 10623 Berlin, Germany. <sup>6</sup>Institute for Biochemistry and Biology, University of Potsdam, Maulbeerallee 2, 14469 Potsdam, Germany. <sup>7</sup>Department of Lake Research, Helmholtz Centre for Environmental Research (UFZ), Brückstr. 3a, 39114 Magdeburg, Germany. <sup>8</sup>Department of Ecology, University of Innsbruck, Technikerstrasse 25, 6020 Innsbruck, Austria. <sup>9</sup>GUT Light Lab, Faculty of Architecture, Gdańsk University of Technology (Gdańsk Tech), Narutowicza 11/12, 80-233 Gdansk, Poland. <sup>10</sup>Institute of Biology, Freie Universität Berlin, Berlin, Germany. ✉email: andreas.jechow@gmx.de

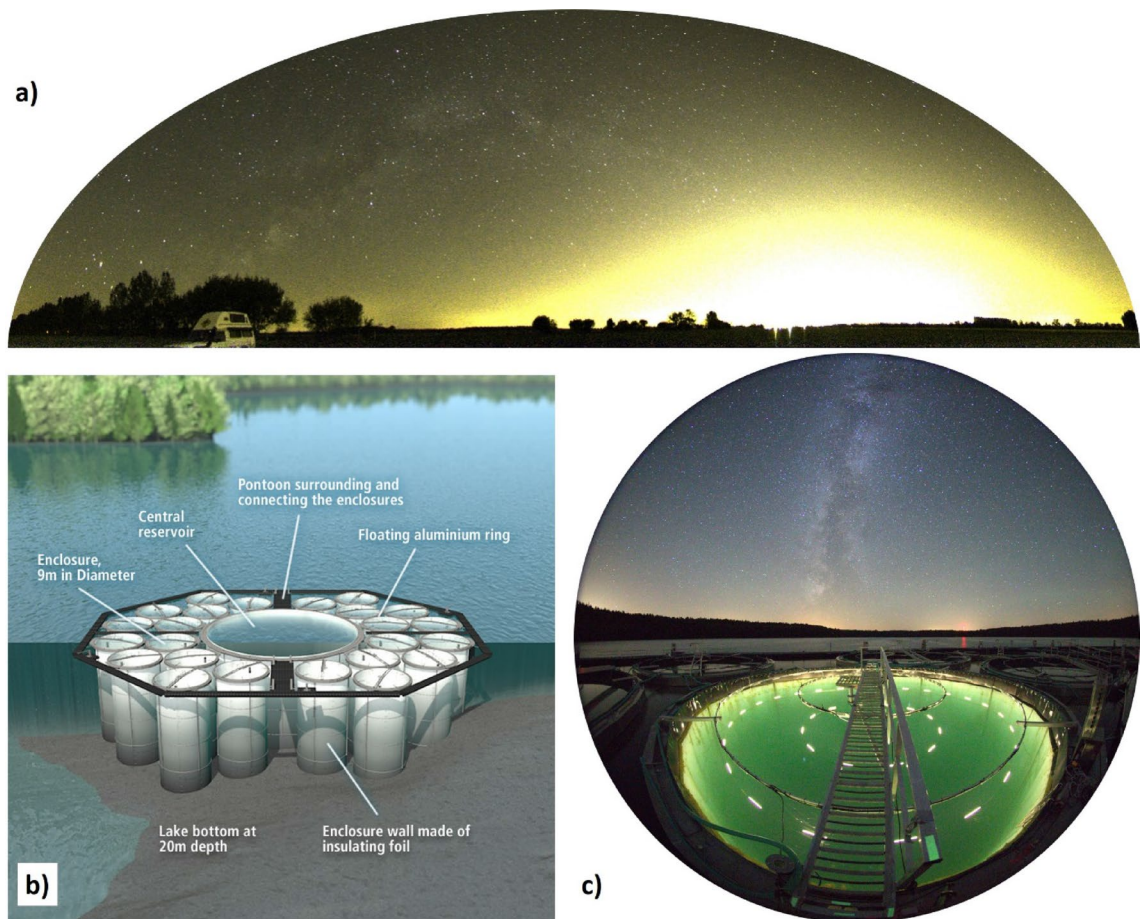


**Figure 1.** The skyglow illumination system. (a) Panoramic image of the skyglow above the city of Berlin, Germany, viewed from 30 km distance obtained from an all-sky image. This image was not taken at the experimental site and serves for illustration purpose of the phenomenon of skyglow. (image credit: A. Jechow) (b) Sketch of the enclosure facility, LakeLab, in Lake Stechlin, Germany (image credit IGB, [www.lake-lab.de](http://www.lake-lab.de)). (c) Skyglow system illuminating one of the enclosures of Lake Lab. The Milky Way and weak skyglow from small towns at the horizon are visible in the background. The green appearance of the water results from backscattering of the LED light. (image credit: A. Jechow).

Artificial skyglow<sup>16</sup> is a form of light pollution which is caused by ALAN being scattered within the atmosphere and redirected back towards the Earth surface<sup>17</sup>. It causes the diffuse glow above illuminated areas such as a large city (Fig. 1a). Skyglow extends over large areas<sup>18</sup> and can be sensed over large distances ranging from several tens to hundreds of km away from the light sources<sup>19,20</sup>. In urban areas, skyglow for clear sky condition can exceed the natural night sky brightness by factors of several tens to hundreds<sup>20–23</sup> resulting in ground illuminances (in the horizontal plane) on the order of 0.01–0.1 lx. Skyglow is dramatically amplified during overcast conditions<sup>20,24</sup> and can then reach extreme night sky brightness values and illuminances of more than 1 lx<sup>20–23</sup>, which is much brighter than moonlight<sup>25</sup>.

Although it is suspected that ecological impacts of skyglow are significant<sup>5–7,26</sup>, experimental studies are scarce. For example, the remarkable sensitivity of the circadian system of several taxa in lab studies, including common freshwater fish<sup>27,28</sup>, indicate that skyglow could influence wild animals over large areas. Another recent study suggests that low skyglow-like ALAN levels disrupt the migration of *Talitrus saltator* (commonly known as sandhoppers), that normally use celestial light at night for orientation<sup>29</sup>. Finally, the amplitude of diel vertical migration of zooplankton can be affected by skyglow, as shown in a seminal experiment conducted in small enclosures deployed in an urban lake<sup>30</sup>.

However, an experimental demonstration of the effects of skyglow in a controlled fashion at a larger scale or at ecosystem level remained elusive so far. Demonstrating ecosystem impacts of environmental stressors requires experiments in realistic settings and of sufficient duration, and the assessment of light pollution effects is no exception. Consequently, experimental test sites have been established to assess consequences of direct ALAN exposures, mainly street lighting<sup>31–33</sup>. Experiments on skyglow, however, are challenging because the spatial light field of the diffuse uniform illumination of skyglow is difficult to emulate, lighting structures shade natural light, and dark experimental control units can be accidentally illuminated<sup>34</sup>. One possible approach is to document ecological responses before and after switching off skyglow sources at the whole-village or city scale. However, such experiments are difficult to implement and virtually impossible to replicate, notably in view of the highly dynamic nature of artificial skyglow resulting from variation in cloud cover<sup>35</sup>, ground albedo<sup>23</sup> or changes in

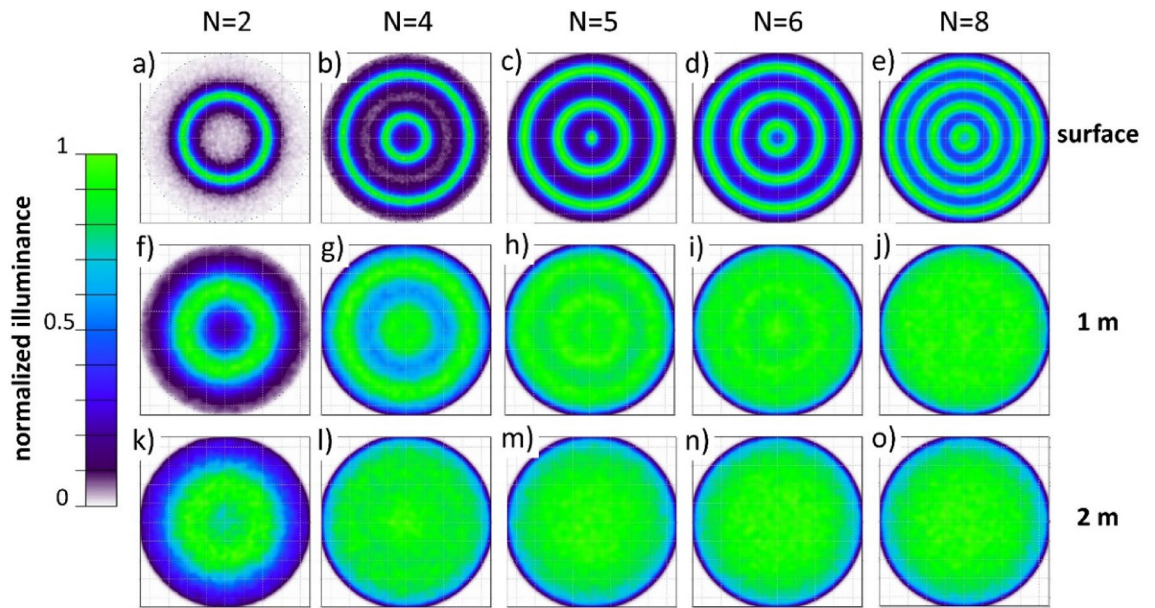


**Figure 2.** Simulation results top view. Modeled horizontal illuminance distribution of the skyglow system for different water depths and for different geometries of ring-shaped light emitters. The upper row (a–e) shows the light distribution at the water surface, the middle row (f–j) the light distribution at 1 m and the lower panels (k–o) at 2 m below the water surface.

urban light emissions<sup>35–37</sup>. Moreover, such experiments can test for recovery from skyglow, the control treatment being the illuminated city, but not on skyglow effects on naïve communities and ecosystems, that never experienced ALAN before. Similar limitations apply to experiments taking advantage of world-wide mass events like the WWF Earth Hour<sup>37</sup>. Thus, city-scale experimental approaches can be valuable to study short-term impacts of skyglow (hour scale), or release thereof, for instance on animal behavior, but cannot inform about long-term consequences on ecosystem-level responses.

Here, we present the first large-scale experimental setup that mimics skyglow realistically at ecosystem level for ALAN naïve communities at a lake enclosure facility located in an area with very low skyglow<sup>18</sup>. The skyglow system was modeled with Monte Carlo raytracing including underwater light propagation and then implemented in the field using concentric rings of light emitting diodes (LEDs) with spatially diffuse emission and a warm-white light spectrum. We outline the rationale behind the design of the skyglow setup and provide details of the implementation and performance of the installation.

## Results

A large-scale experimental enclosure facility implemented in a freshwater lake (Fig. 1b) was illuminated to mimic skyglow (Fig. 1c) on a freshwater ecosystem utilizing state of the art optical modeling. For more information on the facility, the location and its night sky brightness, the experimental requirements, and practical limitations of the skyglow illumination system see Methods section. Figure 1a illustrates the phenomenon of skyglow and was not obtained at the location of the facility, but also near the city of Berlin.

**Modeling the ring geometry: emitters in radial direction.** Given the circular symmetry of the enclosures, a circular shape of the illumination system using a ring-shaped construction was considered most effective. However, given the much more simplistic manufacturing of a rectangular structure, the ring geometry was tested against a rectangular geometry and found to be more effective (Figs. S1, S2). Subsequently, different ring geometries were modeled to find out how many emitters  $N$  across the enclosure diameter are needed for a homogeneous light distribution. The starting parameters for the optical simulation of this arrangement were defined in terms of size of the rings and the number of light emitters  $N$  encountered while crossing the diameter of the enclosure (Fig. S3). In this terminology,  $N=1$  is a single emitter in the center,  $N=2$  is two emitters across the diameter or one ring (Fig. 2a),  $N=3$  is one ring plus a single emitter in the center,  $N=4$  is two rings (Fig. 2b),  $N=5$  is two rings plus a central emitter (Fig. 2c) and so on. The horizontal illuminance distribution for five selected ring geometries with different numbers of emitters  $N$  are shown in Fig. 2. The upper row (a–e) shows the light distribution at the surface, the middle row (f–j) the light distribution at a depth of 1 m and the lower row (k–o) at 2 m depth. In all these models, the whole surface area of each ring is a light emitter, radiating light towards the water surface with the ring-shaped light emitters positioned at  $z=0.4$  m above the water surface.

The homogeneity of the light field created by a single ring (i.e.  $N=2$ ) was largely insufficient (Fig. 2a,f,k), showing a peak-to-valley ratio ( $PVR = E_{max}/E_{min}$ ) of the illuminance at the water surface of  $PVR > 20$ , which reduced to  $PVR \approx 7$  at 1 m depth. The double-ring geometry with  $N=4$  emitters (Fig. 2b,g,l), greatly improved the peak-to-valley ratio to  $PVR \approx 9$  at the surface and to  $PVR \approx 1.5$  at 1 m depth. The addition of a central emitter

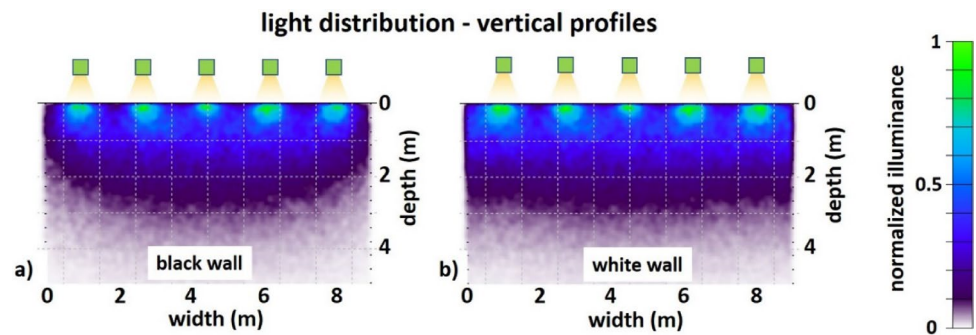


**Figure 3.** Simulation results side-view. Illuminance distribution in the vertical plane for different wall reflectivities. (a) a highly absorbing wall (black), (b) a Lambertian wall with high albedo (white).

to the double-ring geometry with  $N = 5$  (Fig. 2c,h,m) provides an improved peak-to-valley ratio of  $PVR \approx 6$  at the surface and  $PVR \approx 1.3$  at 1 m depth, which is already relatively homogeneous. Adding one more emitter across the diameter with  $N = 6$  (Fig. 2d,i,n) gives only a minor improvement and the four-ring geometry with  $N = 8$  (Fig. 2e,j,o) results in the lowest PVR of about 2 at the surface but only little further improvement at 1 m depth compared to the double ring plus central emitter version ( $N = 5$ ). All solutions apart from  $N = 2$  provide a good homogeneous light field at 2 m depth. These results indicate that the solution with  $N = 5$  is the best compromise of lowest material use, blocking of natural light by providing already a good homogeneity at about 1 m depth.

**Influence of wall albedo.** The spatial light distribution at a given depth does not only depend on scattering and absorption within the bulk water body, but also on losses, reflections and scattering at the enclosure walls. To assess the influence of the wall albedo, we modeled two extreme cases: a black wall that fully absorbs the incident light, and a white wall with 99% Lambertian diffuse reflectance (Fig. 3). Compared to the black absorbing wall (Fig. 3a), the white diffusely reflecting wall (Fig. 3b) improved uniformity of the light field particularly near the edges of the enclosures. This is most apparent at the enclosure walls at a depth lower than 3 m, where the light intensity was lower than in the center of the enclosure when using the black wall (Fig. 3a) but became almost homogeneous in the horizontal plane when using the white wall material (Fig. 3b).

**Emitters in azimuthal direction.** Thus far, the light distribution was segmented only in the radial direction, while in the azimuth direction continuous illumination along the ring-shaped emitters was modeled. However, the simulation of the ring geometry (Fig. 2) showed that an emitter spacing of 1.8 m between the rings will give an acceptable light distribution in the radial direction. Thus, a segmentation of the ring-shaped emitters along the azimuth direction is considered as well. Practical boundaries arise from the length of the emitters and the luminous flux of the LED strips which was 130 lm per m length. The preferred setup with  $N = 5$  emits light from two rings with 3.6 m and 7.2 m in diameter, giving a total length of the light-emitting structure of ca. 34 m which emits a total luminous flux of about 4,400 lm. With the surface area of the enclosure of 64 m<sup>2</sup>, this would result in an average illuminance of 69 lx at the water surface, which is larger than the targeted 0.01–10 lx for the skyglow treatment (see Methods section). The LED strips are available at a minimum length of 27.5 cm and a spacing of 94 cm along the azimuth axis corresponds to 12 emitters for the small and 24 for the large ring plus one central emitter for  $N = 5$ . This segmentation reduces the total emitter length to ca. 10.2 m, the total luminous flux to 1330 lm and the maximum illuminance at the water surface to 21.1 lx, respectively.

The geometry with the 37 emitters was modeled and compared with the original  $N = 5$  full ring geometry (Fig. S4 for direct comparison). Each emitter was implemented in the CAD model and a luminous flux of 36 lm was applied per emitter. The sectioning along the azimuth is clearly perceivable at the water surface (Fig. 4a vs. Figure 2c, also Fig. S4a,b) but the PVR did not increase. At 1 m (Fig. 4b) and 2 m (Fig. 4c) water depth the light distribution with the 37 emitters becomes indistinguishable from the double ring plus central emitter version.

**Testing and optimizing the final setup.** Based on these modeling results and practical considerations (see Methods section), we chose the design with  $N = 5$  and the segmented light emission with 37 total emitters and the white surface for the enclosure walls for the final design of the illumination system. To validate the modeling, we measured the horizontal illuminance with a sensitive underwater luxmeter (ILT 1700 with SUD 33 photopic cosine corrected detector, International Light Technologies, Peabody, USA) at different positions across the diameter of the enclosure at the surface and different depths. The measurements were performed during a moonless night to avoid additional natural light disturbing the result. The natural background was determined to be in the range of the detection limit of the instrument of 0.001 lx. Because of geometrical constraints of the enclosure, the emitters were mounted at slightly different heights, with the large ring closer to the water (25 cm) than the small ring (40 cm) and the central emitter at the largest distance (45 cm). This led to an inhomogeneous intensity distribution for this setup operated at equal luminous flux and without additional wall material (Fig. S5). In this configuration, the illuminance was smallest at the center, largest underneath the large ring and the intensity modulation reached high values of  $PVR \approx 200$  at the water surface. The measured illumi-

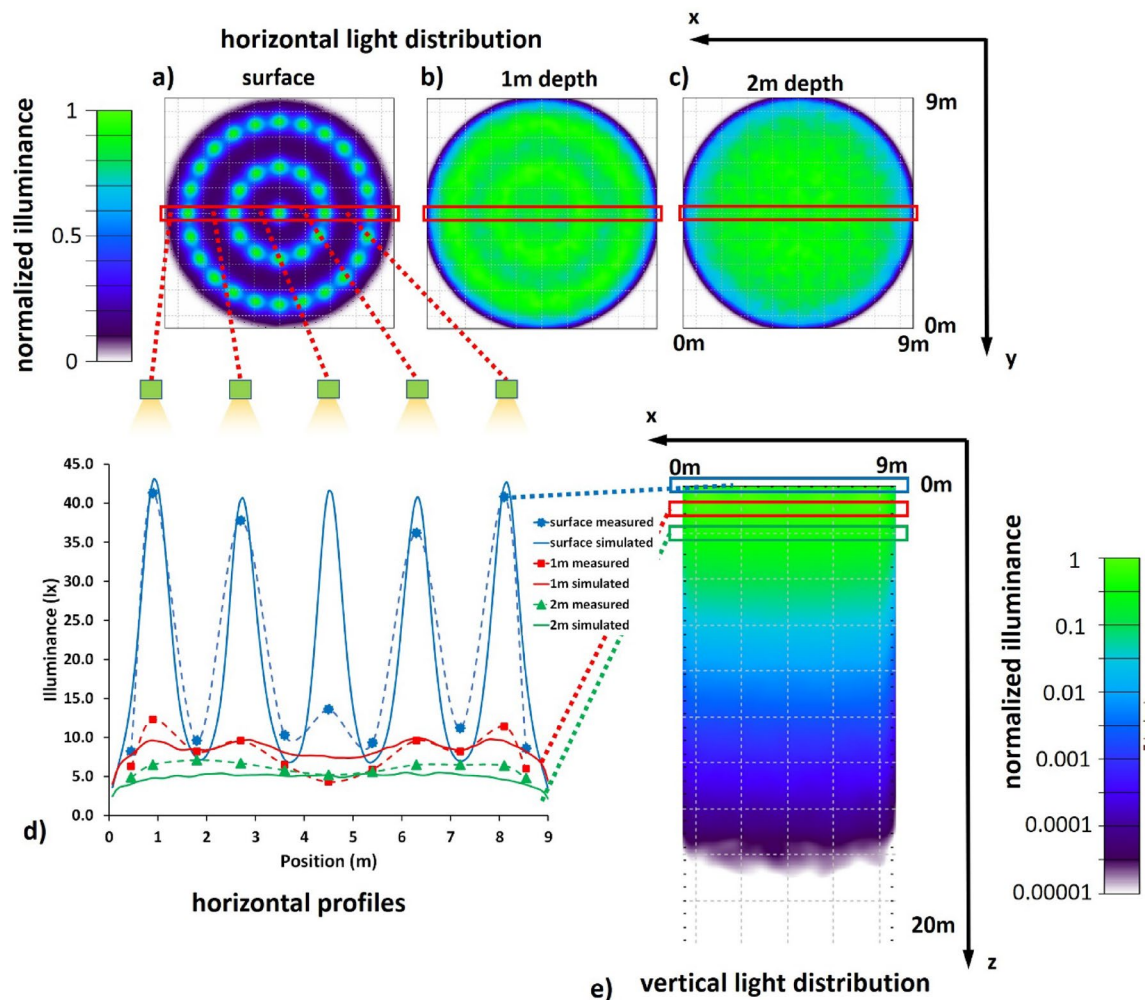


**Figure 4.** Simulation and measurements final design. Illuminance distribution of the final design of the skyglow illumination system simulated for a segmented ring geometry and a total of 37 LED strips: horizontal light distribution (a) at the water surface, (b) 1 m and (c) 2 m below the water surface. (d) horizontal profiles and measured illuminance and (e) vertical light distribution in a cross section of the center of the enclosure down to 20 m depth.

nance of  $21.1 \pm 29.6$  lx at the surface was in the range of the 21 lx estimated beforehand. Even this unoptimized setup showed improved homogeneity at the depths of 1 m ( $PVR \approx 3$ ) and 2 m ( $PVR \approx 2$ ).

Individual dimming adjustments of the LEDs on the large ring and installation of the white wall material improved homogeneity of the light distribution. The measurements and modeling results for this optimized design are plotted in Fig. 4, showing horizontal illuminance distribution at different depths (Fig. 4a–c) and the horizontal illuminance distribution across the enclosure (Fig. 4d) as well as the vertical distribution of the light field (Fig. 4e—note the log scale of the illuminance). The horizontal profiles (Fig. 4d) showed a relatively good match between modeling (solid lines) and measurement results (dashed lines) with a deviation at the central emitter. For this configuration, the illuminance reduced to  $16.9 \pm 12.9$  lx (SD) at the surface. The intensity modulation improved to  $PVR \approx 25$  at the water surface, to  $PVR \approx 2$  at 1 m depth and to  $PVR \approx 1.2$  at 2 m depth.

Further dimming was applied to implement the two skyglow treatments for the experiments with an extreme skyglow treatment at 6 lx and a standard skyglow treatment at 0.06 lx, respectively. Figure 5 shows illuminance measurements obtained with system set to the higher 6 lx skyglow treatment, the results were normalized to 1 for better comparison of homogeneity between different depths. The dimming adjustments resulted particularly in an improved homogeneity at the surface with a measured illuminance of  $6.2 \text{ lx} \pm 4.1 \text{ lx}$  and an improved homogeneity of  $PVR \approx 6$ . At 1 m depth, the homogeneity improved slightly to  $PVR \approx 1.7$  and a near homogeneous light distribution with a  $PVR \approx 1.1$  was achieved at 2 m depth. For the lower skyglow treatment, the system was further dimmed by a factor of 100 (see dimming curve in Fig. S6) and validating by light measurements at a depth of 1 m. Sporadic tests of the light distribution were obtained several times during each of the experiments and checked for plausibility by using measured diffuse attenuation coefficients and comparing illuminance at different depths.

**Practical implementation.** Identical fully functional light sources, consisting of LEDs arranged equidistantly on concentric rings, were installed in all 24 enclosures of the LakeLab (see Fig. 1c for a single enclosure

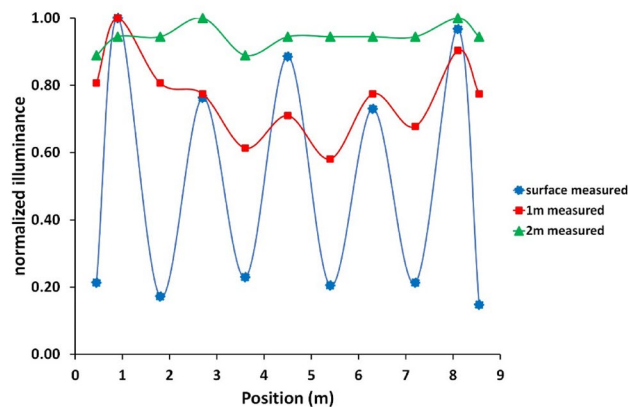


**Figure 5.** Illuminance measurement of final design. Normalized illuminance distribution measured at the surface and 1 m and 2 m water depth for the 6 lx extreme skyglow treatment with adjusted dimming. For numerical values see table S2.



**Figure 6.** The illuminated LakeLab. Aerial photograph of the LakeLab in Lake Stechlin, Germany, with five enclosures each illuminated by high and low levels of emulated skyglow, respectively. (image credit: V. Crone).

and Fig. 6 for an aerial view of the facility). This ensured perfect flexibility in the allocation of treatments to the experimental units and precluded any unintended systematic influences of the illumination system (e.g. leaching of chemicals from the installation) on the experimental outcomes. Instead of “dark” controls, the controls were exposed to natural light<sup>34</sup>. The final design had a double ring geometry (large and small ring plus single central emitter) with 37 emitters per enclosure (see “Results”). None of the 888 LED strips showed any degradation about 3 years after installation outdoors. Light emitters were mounted on an aluminum construction that consisted of rectangular aluminum tube (40 mm height × 20 mm width, with 2.0 mm wall thickness; Fig. S7a) that was bent to the calculated diameters in segments of about 5.6 m length. The metal pieces were cleaned, rinsed, and kept in lake water for several days before joining them to complete rings. The LED strips were attached on land (Fig. S7b) using UV resistant cable ties and an additional aluminum U-profile for extra mechanical support and to provide additional shielding of residual horizontal light. The rings were then transported to the site with a barge (Fig. S7c). The small ring and the central emitter were mounted beneath the bridge spanning across the enclosures (Fig. S7d).

Three electrical circuits were installed to enable individual dimming of the outer and inner ring as well as the central emitter. For each enclosure, a DC power supply (MW LPF-90-24, Meanwell, Taiwan) and a three-channel LED driver were used for dimming and individual control (Vario Contro Linear Drive 180, LEDlinear GmbH, Neukirchen-Vluyn, Germany). Dimming was possible to about 0.01% of the maximum output (Fig. S6). We used an oscilloscope to test for flicker while dimmed, and the modulation frequency was found to be well above 400 Hz even for the extremely low dimming levels. A modular waterproof cable system designed for gardening applications was used (Easy Connect SAS, Toulouse, France) and modified with waterproof shrinking hose.

## Discussion

The illumination system presented here was designed to mimic skyglow at ecosystem-scale within a freshwater enclosure facility. Only a few outdoor and indoor experiments on skyglow have been performed so far. Moore et al.<sup>30</sup> have investigated diel vertical migration of *Daphnia* but did not use an active illumination but rather enclosures that could block or expose the water in the enclosures to the surrounding urban skyglow. This is a seminal experiment, but it lacks a precise characterization of the light field and control over the treatment parameters. Very recently, Torres et al.<sup>29</sup> have investigated the disturbance of a skyglow-like treatment on the migration of *Talitrus saltator* (sandhoppers) that normally use celestial light at night for orientation. They used a confined area at a beach and illuminated it with a single central light source with a warm white spectrum LEDs. They performed light measurements to validate their target of 0.1 lx horizontal illuminance, but the spatial variation of the light field is not provided in their letter. Kupprat et al.<sup>28</sup> used a flexible light system to mimic skyglow-like illumination during the night and daylight in an indoor experiment using medium sized aquaria to test impact of ALAN on melatonin suppression. While the light source is well characterized in terms of spectral and temporal parameters, the spatial light field was not particularly taken care of, which might become important in behavioral and larger scale experiments.

In the work presented here, the aim was to produce a spatially diffuse and homogenous light field as close as possible to real world skyglow. These requirements were largely met by the system relying on LED strips emitting warm-white light with a CCT of 2700 K and a near Lambertian spatial emission pattern.

The size and architecture of the enclosure facility called for a custom solution for the lighting design, while respecting various constraints. A transdisciplinary team of scientists elaborated a solution with valuable input from lighting designers<sup>38</sup>. Optical modeling with raytracing enabled us to produce a tailored solution and to test light sources before purchasing materials and building prototypes or engaging in elaborate measurements. Moreover, a theoretically indefinite number of scenarios differing in geometries and other conditions can be modeled, particularly because modeling makes it possible to simulate optical properties of natural lake water (e.g. regarding scattering and absorption). In principle, the model can thus also accommodate multiple wavelengths with varying scattering and absorption properties. However, since our main objective was to optimize the spatial distribution of the light field, and since the light attenuation in the enclosure water could be effectively measured, it was sufficient to run the models for a single wavelength. Thus, a small number of basic assumptions were sufficient to simulate different geometrical options and devise an optimum solution for our illumination system in terms of optical homogeneity, minimal shading to avoid shielding of natural light, accessibility to the enclosures for sampling, practicality of implementation, and finally costs.

The final design consisted of 37 LED strips each of a length of 27.5 cm that were equally distributed along two supportive ring structures, with one LED strip being mounted at the center of the enclosure. The modeled results indicated only minimally different performance to a full-ring emitter solution (Fig. S4) and an acceptable deviation from the ideal illumination system covering the whole enclosure (see Fig. S2a,d,g). Validation of the modeling results by in situ light measurements above and below the water surface revealed only a slight mismatch between the predicted homogeneity and the measured light field distribution. The desired homogeneity of 1:2 was met at 1 m water depth, and the horizontal homogeneity was excellent at 2 m water depth. However, the light field at the water surface was slightly heterogeneous with a 1:6 intensity modulation. Therefore, any light-induced movements of organisms over small distances at the very top water layer could potentially introduce a bias in experimental results. Still, the model provided exact knowledge about this small weakness and provided potential solution. Finer spacing of the emitters in the radial direction by using a larger number of rings would have resulted in a more homogenous light field at the surface (see Fig. 2) but would compromise our design conditions. Specifically, it would have required more material and raised the building costs and time investment, as well as, most importantly, increase shading of natural light and decrease access to the enclosures for sampling. Thus, we considered our selected final design as the best compromise for the skyglow treatment.

In conclusion, this is the first time that an illumination system to mimic skyglow at ecosystem level has been achieved. Furthermore, precise optical modeling of the spatial light field distribution with physically correct light propagation was utilized for the first time during a design phase of a large-scale experiment. We succeeded in providing a highly homogeneous light field for more than 90% of the experimental volume investigated. While the illumination system itself is highly customized to the freshwater enclosure facility, the method of optical modeling and customization can be adapted to other skyglow experiments both in the laboratory and in the field. This method is particularly useful to aid experimental design for the urgently needed research question on how skyglow effects the environment, by providing exact knowledge of the full light field and by assisting the creation of tailored light distributions.

## Materials and methods

**Study site and facility.** The research infrastructure to be illuminated, the LakeLab (Fig. 1b), is a large-scale experimental enclosure facility installed in Lake Stechlin, Germany. It consists of 24 enclosures, each 9 m in diameter, that are isolated from the open lake by impervious tube-shaped tarpaulin reaching down into the sediment at about 20 m depth<sup>39</sup>. The LakeLab is located 75 km north of the city of Berlin in one of the darkest areas of the country<sup>18</sup>. At this location, clear skies have near-natural brightness, and overcast nights are generally darker than clear nights<sup>40,41</sup>. The location is therefore excellent for testing for effects of skyglow, as the experimental controls are exposed to a near-natural night sky.

**Experimental requirements and limitations.** An ideal light source to mimic skyglow would be a large hemisphere, like a planetarium dome<sup>42</sup>, that emits (or reflects) spatially diffuse radiation. However, such a system is unsuitable for a large outdoor facility, because it blocks natural light during the day and hampers free gas

exchange between the water surface and the atmosphere. Furthermore, the spectrum of skyglow is composed of the spectra of multiple light sources in the first place. Furthermore, these light spectra are altered by being reflected at obstacles (the ground, buildings, vegetation etc.) and subsequently by wavelength dependent scattering within the atmosphere. The spectrum of skyglow will therefore be different at different places on Earth and vary over time, which is too difficult to resemble at an outdoor facility of the scale of LakeLab. Both approaches could however be implemented in future indoor studies. Therefore, acknowledging unavoidable trade-offs, we defined the following experimental requirements:

- A highly diffuse light field with incident light received from nearly all angles
- An intensity modulation better than 2:1 at 1 m depth and nearly homogeneous illumination at 2 m depth
- Light emitters with a nearly uniform (Lambertian) spatial emission pattern
- A light spectrum resembling modern outdoor lighting
- An adjustable illuminance, dimmable within the range of 0.01–10 lx at the water surface
- Minimum blocking of natural light sources such as sunlight, moonlight and starlight
- An open water surface to ensure free gas exchange with the atmosphere
- Easy access to the enclosures to sample water, deploy measurement devices, etc.

Additional practical criteria were suitability for outdoor use, including waterproofness of the light emitters, low power consumption, long lifetime, and low maintenance, electrical and chemical hazard avoidance, and total costs. The rationale behind the illuminance range was that a natural clear night has an illuminance of ca. 0.001 lx, significant skyglow starts at ca. 0.01 lx and extreme skyglow for urban cloudy skies can be more than 1 lx<sup>20</sup>. The target of 10 lx was set because skyglow is increasing exponentially and to have a bit of headroom with the illumination system. Please note that despite lux is an SI unit it is non-ideal for ecological studies, particularly if no spectrum of the light source is provided. For a discussion on this see a recent paper on long-term studies of insects and ALAN<sup>44</sup>.

**LED strips.** We opted for LEDs because they are energy-efficient, can be operated with low Voltage direct current, have excellent dimming properties, and are now widely used for outdoor lighting. LEDs are also available with many spectra and correlated color temperatures (CCTs)<sup>43</sup>. We selected waterproof LED strips (Vari-oLED Flex NIKE LD4 827 SV, LEDlinear GmbH, Neukirchen-Vluyn, Germany) with a warm-white emission spectrum and a CCT of 2700 K (Fig. S8a), which is close to typical CCTs reported for urban light polluted skies in and near Berlin<sup>20</sup>. The manufacturer embedded the LEDs in a scattering matrix, to produce a spatially diffuse light field with a nearly Lambertian (constant apparent brightness independent of observer's position) spatial emission pattern (Fig. S8b). The LED strips were available in lengths between 27.5 cm and 5 m, and had a nominal luminous flux per length of 130 lm/m. In the final design, the shortest length of 27.5 cm was used.

**Raytracing model.** The underwater light field was modeled using the commercial raytracing software TracePro (Version 7.7.1. Lambda Research, Littleton, CO, USA <https://lambdaresearch.com/tracepro/>), which includes physically correct functions for refraction, scattering and absorption. TracePro utilizes non-sequential raytracing based on a Monte-Carlo technique. The software is widely applied to model the propagation of light in tissue, but also used for the design of complex optics or illumination<sup>45</sup>. Monte-Carlo raytracing works by simulating the paths of individual photons (or groups of photons) from a source to some ending position<sup>46</sup>. First, an individual photon is assigned a position in space (x,y,z) corresponding to a source. These starting locations are weighted according to the size and the brightness of the sources, and a position is then randomly chosen according to these weights. Next, the photon is assigned a propagation direction based on the spatial emission properties of the light source. The photon is then taken forward in a set of steps in this direction, until it is either absorbed, experiences a scattering event, or hits a boundary (e.g. a wall, the water surface, or the end of the simulation boundary). At a boundary, the photon's direction is changed, based on the physics of the interaction. Imaginary boundaries may also be inserted into the code to determine the flux of photons at a given location. Photons in the water are scattered via a variety of physical processes, mainly Rayleigh-like scattering from molecules (sometimes also referred to as Einstein–Smoluchowski scattering), and Mie-like scattering from larger water constituents. In a Mie scattering event that dominates in lake water, the photon is diverted to a new trajectory according to a scattering phase function, which is the Henyey–Greenstein function in TracePro:

$$p(\cos \theta) = \frac{1}{2} \frac{1 - g^2}{(1 + g^2 - 2g \cdot \cos \theta)^{3/2}},$$

where  $p(\cos \theta)$  is the probability density function of the cosine of  $\theta$ , with  $\theta$  being the angle relative to the original propagation direction and  $g$  parameterizes the anisotropy of scattering, taking values between +1 and -1 with positive values indicating forward and negative values backward scattering.

TracePro is based on computer aided design (CAD) modeling, which involves first creating the geometrical environment composed of discrete elements, and then applying the appropriate material properties to each of these elements. To model illumination in an enclosure, we thus created a water-filled cylinder of the size of the enclosures (Fig. S9a) adding ring shaped light emitters above the water surface, walls and bottom layers with a specific reflectivity and various detector planes (Fig. S9b). The rays were then propagated through the water in the cylinder (Fig. S9c). The spatial emission pattern of the LED strips (using the photometric data files from the manufacturer, see Fig. S8b) was applied to the lower part of the lighting ring facing the water. Material constants such as the refractive index of water ( $n_{\text{water}} = 1.33$ ) and the absorption coefficient  $\mu_a$  and scattering coefficient  $\mu_s$ ,



were applied to the water-filled cylinder. Although the absorption of pure water is a built-in feature of the software, the optical properties from optically active constituents (phytoplankton, colored dissolved organic matter etc.) of freshwater bodies need to be applied. The modeling parameters were set as follows: the anisotropy factor was  $g = 0.9$  to simulate forward scattering, the scattering coefficient was  $\mu_s = 1/\text{m}$  and the absorption coefficient was  $\mu_a = 0.55/\text{m}$  to represent a wavelength of 500 nm. These values are on the order of previously measured values for the lake<sup>47</sup>, while our own measurements for the diffuse downwelling attenuation coefficient  $k_d$  ranged between 0.3/m and 1.5/m during summer months. Since the focus was on the spatial distribution of light in the enclosures, the modeling was performed for monochromatic light only.

This is plausible because the scattering will not vary as dramatically with wavelength as the absorption in natural freshwaters like Lake Stechlin. In pure water the light scattering coefficient is higher for short wavelengths than for longer wavelengths, similar to Rayleigh scattering within the atmosphere. However, it is in the range of  $\mu_{s,\text{pure}} = 0.01/\text{m}$  for wavelengths above 400 nm<sup>48</sup>. The scattering coefficient from the optical constituents in natural freshwaters in form of organic and inorganic particles will be much higher (we used  $\mu_s = 1/\text{m}$  at 500 nm, which is representative for Lake Stechlin) but will not vary much with wavelength for such water bodies<sup>49</sup>. We tested this for two other wavelengths 400 nm ( $\mu_s = 1.3/\text{m}$ ,  $\mu_a = 0.9/\text{m}$ ) and 600 nm ( $\mu_s = 0.8/\text{m}$ ,  $\mu_a = 0.7/\text{m}$ ) as well as a scenario with strong absorption and relatively low scattering ( $\mu_s = 0.8/\text{m}$ ,  $\mu_a = 3/\text{m}$ ). The results are shown in Fig S10 for 1 m and 2 m depth. Hardly any differences can be perceived for the different wavelengths but a slight deviation at 1 m depth for the strong absorption can be seen. Thus, for a freshwater system like Lake Stechlin, the single wavelength approach is acceptable. However, this can change in strongly absorbing waters and in very turbid waters, where the scattering coefficient can have a stronger wavelength dependency<sup>49</sup>.

## Data availability

All data are available in the main text or the supplementary materials.

Received: 11 August 2021; Accepted: 17 November 2021

Published online: 06 December 2021

## References

- Kyba, C. C. *et al.* Artificially lit surface of Earth at night increasing in radiance and extent. *Sci. Adv.* **3**(11), e1701528 (2017).
- Boyce, P. R. The benefits of light at night. *Build. Environ.* **151**, 356–367 (2019).
- Riegel, K. W. Light pollution: Outdoor lighting is a growing threat to astronomy. *Science* **179**(4080), 1285–1291 (1973).
- Matzke, E. B. The effect of street lights in delaying leaf-fall in certain trees. *Am. J. Bot.* **23**(6), 446–452 (1936).
- Longcore, T. & Rich, C. Ecological light pollution. *Front. Ecol. Environ.* **2**(4), 191–198 (2004).
- Hölker, F., Wolter, C., Perkin, E. K. & Tockner, K. Light pollution as a biodiversity threat. *Trends Ecol. Evol.* **25**(12), 681–682 (2010).
- Gaston, K. J., Visser, M. E. & Hölker, F. The biological impacts of artificial light at night: The research challenge. *Philos. Trans. R. Soc. Lond. B. Biol. Sci.* **370**, 20140133 (2015).
- Schroer, S. & Hölker, F. *Impact of Lighting on Flora and Fauna. Handbook of Advanced Lighting Technology Reference* 1–33 (Springer, New York, 2016).
- Hölker, F. *et al.* Microbial diversity and community respiration in freshwater sediments influenced by artificial light at night. *Philos. Trans. R. Soc. B Biol. Sci.* **370**(1667), 20140130 (2015).
- Robert, K. A., Lesku, J. A., Partecke, J. & Chambers, B. Artificial light at night desynchronizes strictly seasonal reproduction in a wild mammal. *In Proc. R. Soc. B* **282**, 20151745 (2015).
- Knop, E. *et al.* Artificial light at night as a new threat to pollination. *Nature* **548**(7666), 206–209 (2017).
- Kummu, M., de Moel, H., Ward, P. J. & Varis, O. How close do we live to water200A global analysis of population distance to freshwater bodies. *PLoS ONE* **6**(6), e20578 (2011).
- Davies, T. W., Duffy, J. P., Bennie, J. & Gaston, K. J. The nature, extent, and ecological implications of marine light pollution. *Front. Ecol. Environ.* **12**, 347–355 (2014).
- Kurvers, R. H. *et al.* Artificial light at night affects emergence from a refuge and space use in guppies. *Sci. Rep.* **8**(1), 1–10 (2018).
- Jechow, A. & Hölker, F. How dark is a river? Artificial light at night in aquatic systems and the need for comprehensive night-time light measurements. *Wiley Interdiscip. Rev. Water* **6**(6), e1388 (2019).
- Rosebrugh, D. W. Sky-glow from large cities. *J. R. Astron. Soc. Can.* **29**, 79 (1935).
- Aubé, M. Physical behaviour of anthropogenic light propagation into the nocturnal environment. *Philos. Trans. R. Soc. Lond. B Biol. Sci.* **370**, 20140117 (2015).
- Falchi, F. *et al.* The new world atlas of artificial night sky brightness. *Sci. Adv.* **2**(6), e1600377 (2016).
- Kolláth, Z. Measuring and modelling light pollution at the Zselic Starry Sky Park. *J. Phys. Conf. Ser.* **218**(1), 012001 (2010).
- Jechow, A., Kyba, C. C. & Hölker, F. Mapping the brightness and color of urban to rural skyglow with all-sky photometry. *J. Quant. Spectrosc. Radiat. Transf.* **250**, 106988 (2020).
- Kyba, C. C. *et al.* Worldwide variations in artificial skyglow. *Sci. Rep.* **5**, 8409 (2015).
- Pun, C., So, C., Leung, W. & Wong, C. Contributions of artificial lighting sources on light pollution in Hong Kong measured through a night sky brightness monitoring network. *J. Quant. Spectrosc. Radiat. Transf.* **139**, 90–108 (2014).
- Jechow, A. & Hölker, F. Snowglow—the amplification of skyglow by snow and clouds can exceed full moon illuminance in suburban areas. *J. Imaging* **5**(8), 69 (2019).
- Kyba, C. C., Ruhtz, T., Fischer, J. & Hölker, F. Cloud coverage acts as an amplifier for ecological light pollution in urban ecosystems. *PLoS One* **6**(3), e17307 (2011).
- Kyba, C., Mohar, A. & Posch, T. How bright is moonlight. *Astron. Geophys.* **58**, 31–32 (2017).
- Kyba, C. C. M. & Hölker, F. Do artificially illuminated skies affect biodiversity in nocturnal landscapes?. *Landsc. Ecol.* **28**, 1637–1640 (2013).
- Grubisic, M. *et al.* Light pollution, circadian photoreception, and melatonin in vertebrates. *Sustainability* **11**, 6400 (2019).
- Kupprat, F., Hölker, F., & Kloas, W. Can skyglow reduce nocturnal melatonin concentrations in Eurasian perch? *Environ. Pollut.* **262**, 114324 (2020).
- Torres, D., Tidau, S., Jenkins, S. & Davies, T. Artificial Skyglow Disrupts Celestial Migration at Night. *Curr. Biol.* **30**(12), 696–697 (2020).
- Moore, M. V., Pierce, S. M., Walsh, H. M., Kvalvik, S. K. & Lim, J. D. Urban light pollution alters the diel vertical migration of *Daphnia*. *Internationale Vereinigung für theoretische und angewandte Limnologie: Verhandlungen* **27**(2), 779–782 (2000).

31. Bennie, J., Davies, T. W., Cruse, D., Inger, R. & Gaston, K. J. Cascading effects of artificial light at night: Resource-mediated control of herbivores in a grassland ecosystem. *Philos. Trans. R. Soc. Lond. B Biol. Sci.* **370**(1667), 20140131 (2015).
32. Spoelstra, K. *et al.* Experimental illumination of natural habitat—an experimental set-up to assess the direct and indirect ecological consequences of artificial light of different spectral composition. *Philos. Trans. R. Soc. B Biol. Sci.* **370**(1667), 20140129 (2015).
33. Holzhauer, S. I. *et al.* Out of the dark: Establishing a large-scale field experiment to assess the effects of artificial light at night on species and food webs. *Sustainability* **7**(11), 15593–15616 (2015).
34. Walbeek, T. J., Harrison, E. M., Gorman, M. R. & Glickman, G. L. Naturalistic intensities of light at night: A review of the potent effects of very dim light on circadian responses and considerations for translational research. *Front. Neur.* **12**, 27 (2021).
35. Jechow, A. *et al.* Tracking the dynamics of skyglow with differential photometry using a digital camera with fisheye lens. *J. Quant. Spectrosc. Radiat. Transf.* **209**, 212–223 (2018).
36. Barentine, J. C. *et al.* Recovering the city street lighting fraction from skyglow measurements in a large-scale municipal dimming experiment. *J. Quant. Spectrosc. Radiat. Transf.* **253**, 107120 (2020).
37. Jechow, A. Observing the impact of WWF earth hour on urban light pollution: A case study in Berlin 2018 using differential photometry. *Sustainability* **11**(3), 750 (2019).
38. Pérez Vega, C., Zielinska-Dabkowska, K. M. & Hölker, F. Urban lighting research transdisciplinary framework—a collaborative process with lighting professionals. *Int. J. Environ. Res. Public Health* **18**(2), 624 (2021).
39. Giling, D. P. *et al.* Thermocline deepening boosts ecosystem metabolism: Evidence from a large-scale lake enclosure experiment simulating a summer storm. *Glob. Change Biol.* **23**(4), 1448–1462 (2017).
40. Jechow, A., Hölker, F., Kollath, Z., Gessner, M. O. & Kyba, C. C. M. Evaluating the summer night sky brightness at a research field site on Lake Stechlin in northeastern Germany. *J. Quant. Spectrosc. Radiat. Transf.* **181**, 24–32 (2016).
41. Jechow, A., Hölker, F. & Kyba, C. C. M. Using all-sky differential photometry to investigate how nocturnal clouds darken the night sky in rural areas. *Sci. Rep.* **9**(1), 1–14 (2019).
42. Dacke, M., Baird, E., Byrne, M., Scholtz, C. H. & Warrant, E. J. Dung beetles use the milky way for orientation. *Curr. Biol.* **23**, 298–300 (2013).
43. Zielinska-Dabkowska, K. M. Make lighting healthier. *Nature* **553**, 274–276 (2018).
44. Kalinkat, G. *et al.* Assessing long-term effects of artificial light at night on insects: What is missing and how to get there. *Insect Conserv. Divers.* **14**(2), 260–270 (2021).
45. Su, Z., Xue, D. & Ji, Z. Designing led array for uniform illumination distribution by simulated annealing algorithm. *Opt. Express* **20**, A843–A855 (2012).
46. Jacques, S. L. & Wang, L. *Monte Carlo Modeling of Light Transport in Tissues* 73–100 (Springer, New York, 1995).
47. Göritz, A. *et al.* Retrieval of Water constituents from hyperspectral in-situ measurements under variable cloud cover—a case study at Lake Stechlin (Germany). *Remote Sens.* **10**(2), 181 (2018).
48. Mobley, C. D. & Mobley, C. D. *Light and Water: Radiative Transfer in Natural Waters* (Academic Press, New York, 1994).
49. Gould, R. W., Arnone, R. A. & Martinolich, P. M. Spectral dependence of the scattering coefficient in case 1 and case 2 waters. *Appl. Opt.* **38**(12), 2377–2383 (1999).

## Acknowledgements

We thank the whole ILES consortium comprising a multi-national team of scientists, lighting experts and engineers; the technical staff at IGB Stechlin, particularly Gonzalo Idoate Santaolalla and Ignacio Ajamil Rodanes for help with building and installing the skyglow system and the Loss of the Night network for valuable discussions about skyglow.

## Author contributions

A.J. coordinated the design and implementation of the illumination system and performed the raytracing simulation together with G.S. A.J., G.S., and C.C.M.K. designed the illumination system with input from K.Z.D., S.A.B., M.O.G., H.P.G., F.K., J.C.N., T.S., G.A.S., S.S., T.J.W., S.W., and F.H. K.Z.D. suggested the LED illuminant. A.J., G.S., M.B., Ar.P., M.S., and T.J.W. constructed and tested a prototype. S.A.B. designed and S.A.B., G.S., and S.S. built the mobile white enclosure wall. A.J., G.S., C.C.M.K., L.T.B., M.B., M.S., F.K., An.P., and T.J.W. built and installed the illumination system. A.J., G.S., C.C.M.K., and F.H. performed the light measurements in the field. A.J. wrote the first draft of the manuscript. All authors provided feedback on intermediate drafts and approved the final version.

## Funding

Open Access funding enabled and organized by Projekt DEAL. This work was part of the Illuminating Lake Ecosystems (ILES) project funded by the Leibniz Association (SAW-2015-IGB-1). Further support was received through the projects Bridging in Biodiversity Science (BIBS) funded by the German Federal Ministry of Education and Research (BMBF, grant no. 01LC1501G), a core facility grant provided by the German Research Foundation (DFG, GE 1775/2–1), and a grant by the BMBF for building the enclosure facility (033L041B). AJ was partly supported by IGB's Frontiers in Freshwater Science program.

## Competing interests

The authors declare no competing interests.

## Additional information

**Supplementary Information** The online version contains supplementary material available at <https://doi.org/10.1038/s41598-021-02772-4>.

**Correspondence** and requests for materials should be addressed to A.J.

**Reprints and permissions information** is available at [www.nature.com/reprints](http://www.nature.com/reprints).

**Publisher's note** Springer Nature remains neutral with regard to jurisdictional claims in published maps and institutional affiliations.



**Open Access** This article is licensed under a Creative Commons Attribution 4.0 International License, which permits use, sharing, adaptation, distribution and reproduction in any medium or format, as long as you give appropriate credit to the original author(s) and the source, provide a link to the Creative Commons licence, and indicate if changes were made. The images or other third party material in this article are included in the article's Creative Commons licence, unless indicated otherwise in a credit line to the material. If material is not included in the article's Creative Commons licence and your intended use is not permitted by statutory regulation or exceeds the permitted use, you will need to obtain permission directly from the copyright holder. To view a copy of this licence, visit <http://creativecommons.org/licenses/by/4.0/>.

© The Author(s) 2021